INTERFACE

royalsocietypublishing.org/journal/rsif

Research

Cite this article: Krewing M *et al*. 2019 The molecular chaperone Hsp33 is activated by atmospheric-pressure plasma protecting proteins from aggregation. *J. R. Soc. Interface* **16**: 20180966.
http://dx.doi.org/10.1098/rsif.2018.0966

Received: 21 December 2018
Accepted: 24 May 2019

Subject Category:
Life Sciences–Physics interface

Subject Areas:
biochemistry, medical physics, biomedical engineering

Keywords:
chaperone, plasma resistance, non-equilibrium plasma, dielectric barrier discharge, atmospheric-pressure plasma

Author for correspondence:
Julia E. Bandow
e-mail: julia.bandow@rub.de

†These authors equally contributed to the manuscript.
‡Present address: Leibniz Institute for Plasma Science and Technology (INP) Greifswald, Germany.

Electronic supplementary material is available online at https://dx.doi.org/10.6084/m9.figshare.c.4531724.

THE ROYAL SOCIETY PUBLISHING

The molecular chaperone Hsp33 is activated by atmospheric-pressure plasma protecting proteins from aggregation

Marco Krewing[1,†], Jennifer Janina Stepanek[1,†], Claudia Cremers[4], Jan-Wilm Lackmann[1,‡], Britta Schubert[1], Alexandra Müller[2], Peter Awakowicz[3], Lars I. O. Leichert[2], Ursula Jakob[4] and Julia E. Bandow[1]

[1]Applied Microbiology, Faculty of Biology and Biotechnology, [2]Microbial Biochemistry, Faculty of Medicine, and [3]Electrical Engineering and Plasma Technology, Faculty of Electrical Engineering and Information Sciences, Ruhr University Bochum, Bochum, Germany
[4]Molecular, Cellular, and Developmental Biology, University of Michigan, Ann Arbor, MI, USA

MK, 0000-0002-5315-8755; J-WL, 0000-0001-8182-8034; LIOL, 0000-0002-5666-9681; JEB, 0000-0003-4100-8829

Non-equilibrium atmospheric-pressure plasmas are an alternative means to sterilize and disinfect. Plasma-mediated protein aggregation has been identified as one of the mechanisms responsible for the antibacterial features of plasma. Heat shock protein 33 (Hsp33) is a chaperone with holdase function that is activated when oxidative stress and unfolding conditions coincide. In its active form, it binds unfolded proteins and prevents their aggregation. Here we analyse the influence of plasma on the structure and function of Hsp33 of *Escherichia coli* using a dielectric barrier discharge plasma. While most other proteins studied so far were rapidly inactivated by atmospheric-pressure plasma, exposure to plasma activated Hsp33. Both, oxidation of cysteine residues and partial unfolding of Hsp33 were observed after plasma treatment. Plasma-mediated activation of Hsp33 was reversible by reducing agents, indicating that cysteine residues critical for regulation of Hsp33 activity were not irreversibly oxidized. However, the reduction yielded a protein that did not regain its original fold. Nevertheless, a second round of plasma treatment resulted again in a fully active protein that was unfolded to an even higher degree. These conformational states were not previously observed after chemical activation with HOCl. Thus, although we could detect the formation of HOCl in the liquid phase during plasma treatment, we conclude that other species must be involved in plasma activation of Hsp33. *E. coli* cells over-expressing the Hsp33-encoding gene *hslO* from a plasmid showed increased survival rates when treated with plasma while an *hslO* deletion mutant was hypersensitive emphasizing the importance of protein aggregation as an inactivation mechanism of plasma.

1. Introduction

Plasma medicine is an emerging field that covers applications of technical plasmas in biology and medicine. The antibacterial properties of plasmas are exploited for the treatment of materials, devices [1,2] and patients [3,4]. The antibacterial effects are based in part on plasma-generated reactive oxygen and nitrogen species [5], to which microorganisms are reportedly more susceptible than eukaryotic cells [4]. The mechanisms that contribute to inactivation of microorganisms by plasma are manifold and modifications of different biomolecules have been observed. This includes proteins [6], DNA [7], lipids [8], carbohydrates [9], and low molecular weight compounds [10].

Proteins are among the most abundant macromolecules in cells and analyses on the influence of plasma on proteins revealed that most proteins are inactivated within seconds or minutes [11–14]. This is the case even for proteins

that are otherwise known for their high stability like RNase A or proteinase K [15,16]. Oxidation of the sulfur-containing amino acids cysteine and methionine are typically the first plasma-induced modifications, followed by alterations of tryptophan, tyrosine, or histidine [15,17,18]. If the modified residues are part of the catalytic centre, inactivation occurs before changes in tertiary structure are observed [6]. Apart from that, modifications of residues of structural importance can lead to partial or complete protein unfolding and thus to a complete loss of activity [6,11,12]. A noteworthy exception to plasma-mediated inactivation of proteins is the activation of a fungal lipase from *Candida rugosa*. This enzyme unfolds during plasma treatment resulting in an increased catalytic activity. It is thought that the unfolding allows better access of the substrate to the catalytic centre [19].

Denatured and unfolded proteins tend to stick together and form insoluble and lethal protein aggregates [20]. This has also been observed after exposure of *Saccharomyces cerevisiae* yeast cells to atmospheric-pressure plasma as determined by protein quantitation and SDS-PAGE analysis. Plasma-generated hydrogen peroxide (H_2O_2) was shown to be at least partially responsible for this effect [21]. Heat shock proteins and molecular chaperones like $Hsp104_{Sc}$ and $Tsa1_{Sc}$, respectively, were found to be upregulated in yeast after treatment with sublethal plasma doses emphasizing the importance of protein unfolding and aggregation under plasma-induced stress [21].

The heat shock protein 33 (Hsp33) of *Escherichia coli* is a molecular chaperone that ATP-independently binds to unfolded proteins and prevents protein aggregation [22]. Hsp33 is activated by oxidation at elevated temperatures and prevents lethal protein aggregation in bacteria under these conditions [23,24]. It harbours six cysteine residues, four of which are highly conserved and involved in the coordination of a zinc ion [25,26]. Under oxidative stress, these cysteines engage in disulfide bonds leading to the release of the zinc ion. Under conditions that promote unfolding, like elevated temperature, a linker region within the protein unfolds resulting in complete activation of Hsp33 [23,27]. Hsp33 is activated by a combination of the slow-acting oxidant H_2O_2 in conjunction with protein unfolding conditions (e.g. oxidative heat stress), or by exposure to fast-acting protein unfolding oxidants, such as hydroxyl radicals or hypochlorous acid (HOCl) [22,24,25,28].

Cold atmospheric-pressure plasmas contain a number of reactive species potentially capable of activating Hsp33 like different ions, metastables, radicals, and photons. When driven with ambient air as feed gas, reactive oxygen species (ROS) like singlet oxygen ($^1\Delta_gO_2$) and atomic oxygen (•O), as well as several reactive nitrogen species, e.g. N_xO_y or excited nitrogen ($N_2(A^3\Sigma)$), are generated [29]. Some of these particles enter the liquid phase, where they recombine to form species like H_2O_2 or peroxynitrite ($ONOO^-$) [30]. The formation of HOCl, a potent disinfectant known from household bleach, has been predicted based on simulations of plasma treatment of solutions containing chloride ions. Further, HOCl was detected experimentally in leukaemia cell lines after exposure to a He/O_2 plasma jet [31]. It has been postulated that plasma-generated atomic oxygen enters the liquid phase and reacts with chloride ions to yield hypochlorite (OCl^-) [31,32]. Only recently, using $^{18}O_2$ in the feed gas of a plasma jet, it was shown that plasmas can be an effective source of atomic oxygen that enters the liquid phase reacting with solutes [33].

As Hsp33 is known to protect cells from oxidative damage caused by H_2O_2 and HOCl, and both are common species in plasma-treated liquids, we investigated the role of Hsp33 in plasma resistance and the effects of plasma on Hsp33 structure and activity. Studying the effects of plasma treatment on Hsp33 and *E. coli* as a whole, we found that plasma treatment turns Hsp33 into an active chaperone that *in vitro* prevents protein aggregation and contributes to plasma resistance of *E. coli*.

2. Results

2.1. Hsp33 protects *E. coli* against plasma toxicity

Plasma treatment is known to cause oxidative stress and protein denaturation [21], while the molecular chaperone Hsp33 has been shown to protect proteins against oxidative protein unfolding and aggregation [22]. We therefore decided to test whether Hsp33 is activated by plasma, and to what extent Hsp33 protects *E. coli* against plasma toxicity. We exposed *E. coli* wild-type [34], the Hsp33 deletion strain (*ΔhslO*) [34] and the complemented *ΔhslO* strain expressing His_6-tagged Hsp33 IPTG-dependently from a plasmid [35] to DBD-generated plasma. Five microlitres of diluted cell suspension (8×10^4 CFU ml^{-1}, or 400 CFU total) was treated with plasma for 30 s, subsequently plated on LB agar, and CFUs counted after overnight incubation at 37°C. The *E. coli* parent strain exhibited a survival rate of about 55%. The survival rate of the *hslO* deletion strain was decreased to 35%, while that of the complemented *ΔhslO* strain induced with 100 µM IPTG was increased to 70% (figure 1). Although modest, these results suggest that Hsp33 has a cytoprotective effect towards plasma treatment and that the presence or absence of the *hslO* gene is a genetic determinant of plasma resistance of *E. coli*. In order to correlate survival rates with Hsp33 levels, a western blot analysis was conducted to detect Hsp33 expressed from the plasmid with an antibody directed at the His-tag (figure 1, insert). We detected Hsp33 expression only at the highest IPTG concentration (100 µM), congruent with the lack of protective effects at lower inducer levels.

2.2. Hsp33 delays plasma-induced protein aggregation

To investigate the role of Hsp33 in preventing plasma-triggered protein aggregation, *in vitro* assays were performed. Cell lysates of *E. coli* were treated with the DBD with and without the addition of defined amounts of purified Hsp33. After plasma treatment, soluble proteins were separated from aggregated proteins by centrifugation. Proteins in the supernatant and pellet fractions were analysed by SDS-PAGE (figure 2*a*,*b*) and protein quantitation using the Bradford assay (figure 2*c*). Starting from 2 min, proteins were detected in the pellet fraction. After 10 min of plasma treatment, all protein was insoluble. We observed an accumulation of high molecular weight complexes in the pellet fraction that were not solubilized by SDS, suggesting that protein is irreversibly cross-linked. Moreover, the decrease in total signal intensity per sample indicated that plasma causes protein degradation.

When purified Hsp33 was added to the lysate prior to plasma exposure, much less protein aggregated after 5 min of plasma treatment. Seventy per cent of the protein was

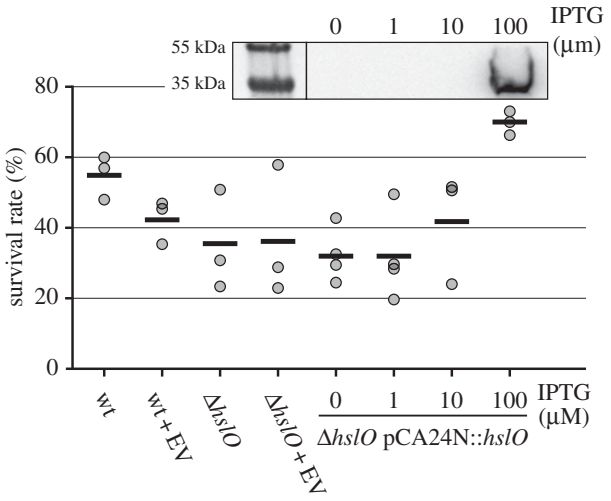

Figure 1. Survival of *E. coli* strains upon exposure to DBD as determined in a CFU-based assay. The tested strains included the parental wild-type strain (wt), the corresponding deletion mutant *ΔhslO*, both with or without the empty vector (EV) pCA24N and the complemented strain *ΔhslO* pCA24N::*hslO* cultivated with different IPTG concentrations. Each dot represents an independent experiment, horizontal lines mark the arithmetic mean. Insert: Samples from strains carrying the plasmid with the His-tagged *hslO* gene were analysed by western blot with anti-His_5-antibody. For each lane, 10 μg protein were applied. The PageRuler Plus prestained protein ladder (Thermo Fisher) was used as size marker.

still soluble, compared to only 15% in samples with no added Hsp33 (figure 2*c*). These results revealed that Hsp33 protects against and delays plasma-induced protein aggregation. Moreover, we detected less cross-linked protein (high molecular mass signals) in the insoluble fraction in the samples with added Hsp33.

2.3. Plasma-induced activation of Hsp33 *in vitro*

To act as a molecular chaperone, Hsp33 needs to be activated by oxidative disulfide bond formation and partial unfolding [23]. We therefore investigated plasma-induced activation of Hsp33, monitored the oxidation status of Hsp33 thiols and investigated protein conformation by circular dichroism (CD) spectroscopy.

Chaperone activity of Hsp33 was determined using the citrate synthase assay after exposure to DBD plasma for up to 2 min (figure 3*a*). As described previously, HOCl-activated Hsp33 prevented citrate synthase aggregation so that no light scattering was observed [24]. Sixty seconds of plasma treatment activated Hsp33 to almost the same extent as treatment with a 10-fold molar excess of HOCl (figure 3*a*).

Upon HOCl-activation, the four conserved thiols form two disulfide bonds and release the zinc ion [24]. To monitor the thiol oxidation status in Hsp33 upon plasma treatment, we conducted an Ellman's assay [36] (figure 3*b*). Consistent with the observed plasma activation of Hsp33, the number of free thiols decreased with increasing plasma exposure, and no remaining free thiol groups were detectable after 60 s of exposure.

Since oxidative activation of Hsp33 is known to be accompanied by massive structural rearrangements, we analysed the secondary structure of Hsp33 using far-UV CD spectroscopy (figure 3*c*). After 45 s of plasma treatment, the degree of Hsp33 unfolding was comparable to HOCl-activated Hsp33. Prolonged exposure for up to 120 s,

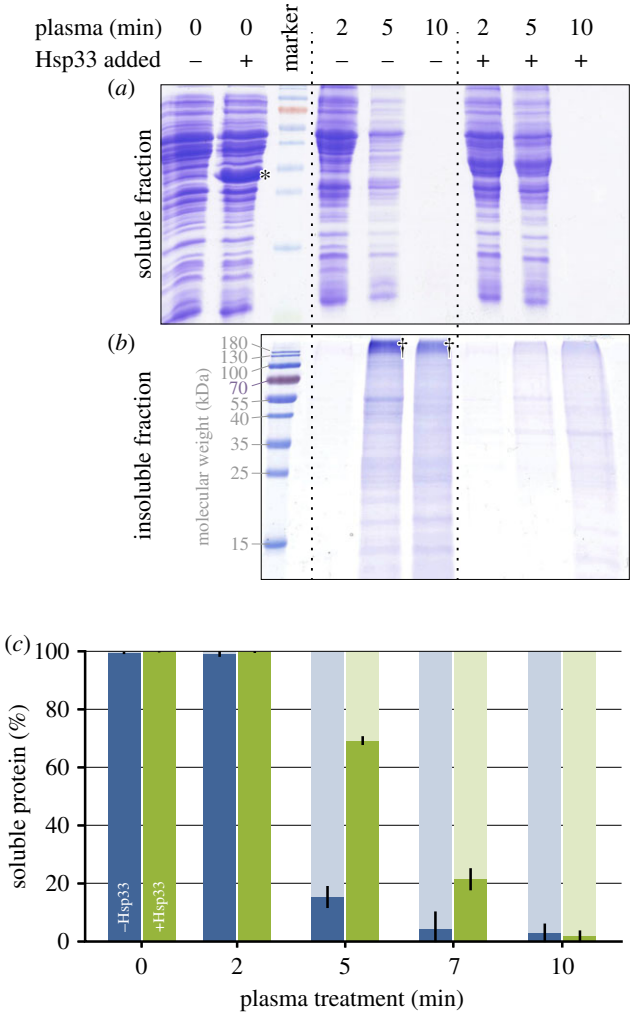

Figure 2. Cell lysates of *E. coli* with (+) or without (−) exogenous Hsp33 (16% (w/w)) were treated with plasma for the indicated amount of time. Insoluble proteins were separated from soluble proteins by centrifugation and both fractions were subjected to SDS-PAGE (*a*,*b*) and Bradford analysis (*c*). (*a*) Soluble protein remaining in the supernatant after plasma treatment. (*b*) Insoluble protein in the pellet fraction. †High molecular mass protein aggregates; *the band to the left corresponds to added Hsp33. The data shown are representative of four independent experiments. (*c*) Bradford quantitation of the protein fractions. Blue bars (left) represent samples without added Hsp33, green bars (right) those to which 16% (w/w) Hsp33 was added prior to plasma treatment. Solid bars (dark): soluble proteins, shaded bars (light): insoluble fraction. For each time point, the total amount of protein (soluble plus insoluble) was set to 100%. The data reflect the results of three independent experiments and standard deviation. (Online version in colour.)

however, resulted in an even more pronounced unfolding of the protein. These additional changes were accompanied by only minor changes in the activity of $Hsp33_{Plasma}$ (compare figure 3*a* and 3*c*).

2.4. Reversibility of plasma-induced Hsp33 activation

Activation of Hsp33 by HOCl is reversible, once reducing conditions are restored and free zinc ions are provided [24]. The fact that the degree of protein unfolding increased with increasing plasma exposure time prompted us to investigate the reversibility of plasma activation of Hsp33. We found that Hsp33 treated for 45, 60, or 120 s ($Hsp33_{P45}$, $Hsp33_{P60}$, and $Hsp33_{P120}$) was fully inactivated after incubation with the reducing agent dithiothreitol (DTT) and addition of

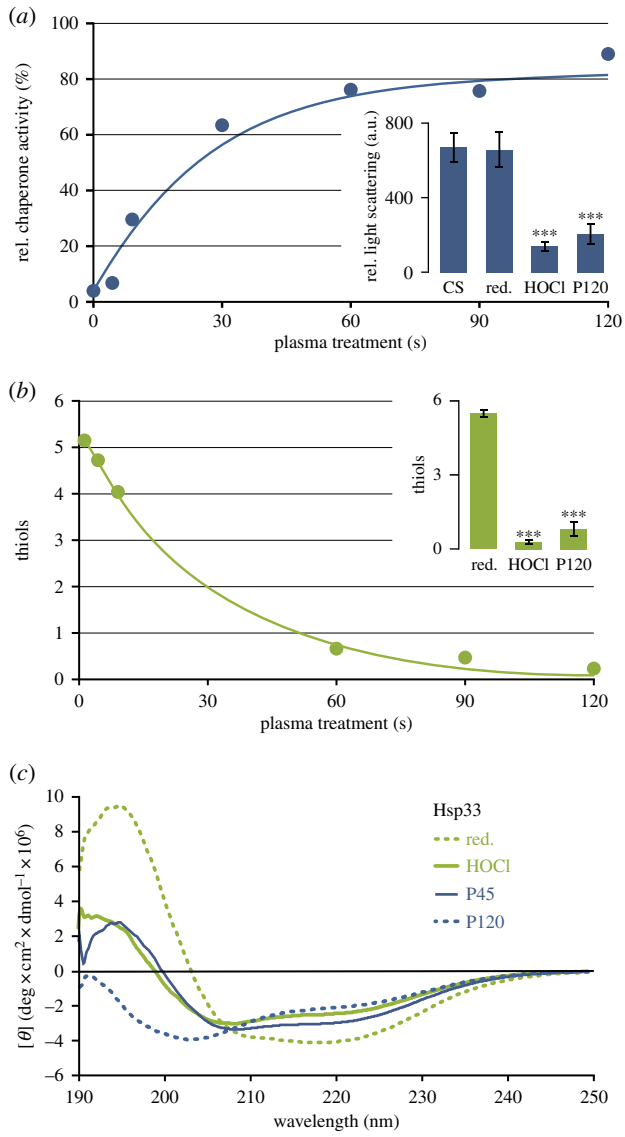

Figure 3. *In vitro* characterization of Hsp33 treated with DBD plasma. (*a*) Relative chaperone activity of plasma-exposed Hsp33 compared to HOCl-treated Hsp33 (set to 100%). Active chaperone prevents the aggregation of citrate synthase resulting in low light scattering. Insert: Light scattering in the citrate synthase assay for citrate synthase alone (CS), in the presence of reduced Hsp33 (red), HOCl-activated Hsp33 (HOCl) or Hsp33 treated with plasma for 120 s (P120). Data shown in insert reflect three independent experiments. (*b*) Average number of free thiols per Hsp33 molecule after plasma treatment quantified with Ellman's reagent. Insert: Comparison of free thiols in HOCl and plasma-treated Hsp33. Data shown in insert reflect three independent experiments. (*c*) Far-UV CD spectra of reduced, HOCl-activated Hsp33, and Hsp33 treated with plasma for 45 or 120 s (P45 and P120, respectively). Inserts in (*a*,*b*): the significance of differences compared to reduced Hsp33 was calculated using Student's *t*-test (***denotes $p \leq 0.001$). (Online version in colour.)

$ZnCl_2$ (figure 4*a*,*b*). Inactivation rates were slightly lower for $Hsp33_{P120}$ (figure 4*a*). While the reduction of $Hsp33_{HOCl}$ yielded the expected six free cysteines, we detected on average only 4.5 thiols in $Hsp33_{P45\text{-}red}$, indicating that during plasma treatment one or two cysteine residues are oxidized to a degree that is not reducible by DTT (like sulfinic or sulfonic acids). We further tested it after the reduction (i.e. inactivation) with DTT, $Hsp33_{HOCl}$ and $Hsp33_{P45}$ could be re-activated with HOCl or plasma, respectively. When Hsp33 was activated by HOCl, inactivated with DTT, and then re-activated by HOCl, the protein unfolded, refolded, and unfolded again, fully in congruence with the chaperone activity data (figure 4*c*). By contrast, as described above, reduction of plasma-activated Hsp33 did not lead to refolding yet also resulted in an inactive protein (figure 4*d*). When this $Hsp33_{P45\text{-}red}$ was then treated with plasma again, chaperone activity returned and we observed an even higher degree of unfolding, which was almost comparable to that after a single treatment for 120 s (compare figure 4*d* and figure 3*b*). This additive effect on the protein unfolding suggested that some plasma-induced protein modifications accumulated that could not be restored by incubation with DTT.

2.5. Role of plasma-generated HOCl in the activation of Hsp33

Hsp33 is activated by H_2O_2 in combination with heat, by hydroxyl radicals or, most effectively, by HOCl [22,24,25,28]. Plasma consists of a variety of reactive species and additional species are produced in plasma-treated aqueous solutions, including those known to activate Hsp33 [30].

In a first attempt to identify the plasma-generated species that activated Hsp33, we investigated HOCl generation using hydroxyphenyl fluorescein (HPF) and aminophenyl fluorescein (APF). Both of these reagents react with hydroxyl radicals and peroxynitrite, but only APF also reacts with HOCl [37]. When treating APF or HPF-containing buffers (storage buffer of Hsp33, 40 mM KH_2PO_4, with or without 20 mM KCl, pH 7.5) with plasma, fluorescence increased equally fast for both probes independent of chloride content and maximal fluorescence was achieved for both probes at 15 s exposure time.

Since it is unknown if the probes also react with highly reactive short-living species from plasma, we also added the probes *after* exposing the buffer solutions to plasma. Under these conditions, we found significant differences in the signals between both probes, indicative of the formation of HOCl when chloride ions are present. We then compared the fluorescence signals of the two probes dissolved in chloride-containing or chloride-free buffer after exposure to plasma and calculated the HOCl concentrations as described in the materials and methods section. After a 30 s treatment with the DBD, we detected 0.9 µM HOCl in the chloride-containing buffer solution (electronic supplementary material, figure S1). Given that optimal Hsp33 activation requires at least a 10 : 1 ratio of HOCl to Hsp33, these results suggested that plasma-induced HOCl production is not sufficient to activate Hsp33 present at 150 µM. Since during the plasma treatment the solutions did not contain Hsp33, we cannot exclude that more HOCl is generated when Hsp33 acts as a sink for HOCl during the plasma treatment.

After verifying that HOCl is formed in DBD-treated liquid, the contribution of HOCl in the plasma-induced activation of Hsp33 was analysed. To this end, chloride-containing buffer was exposed to the DBD plasma for 120 s and subsequently mixed with an Hsp33 solution. This procedure allows highly reactive short-living species like hydroxyl radicals or singlet oxygen (life times: microsecond- to millisecond-range) [38,39] to decay. HOCl is reported to be relatively stable [40]. No Hsp33 activation was observed after a 10 min incubation with a buffer that was treated with plasma for 2 min (electronic supplementary material,

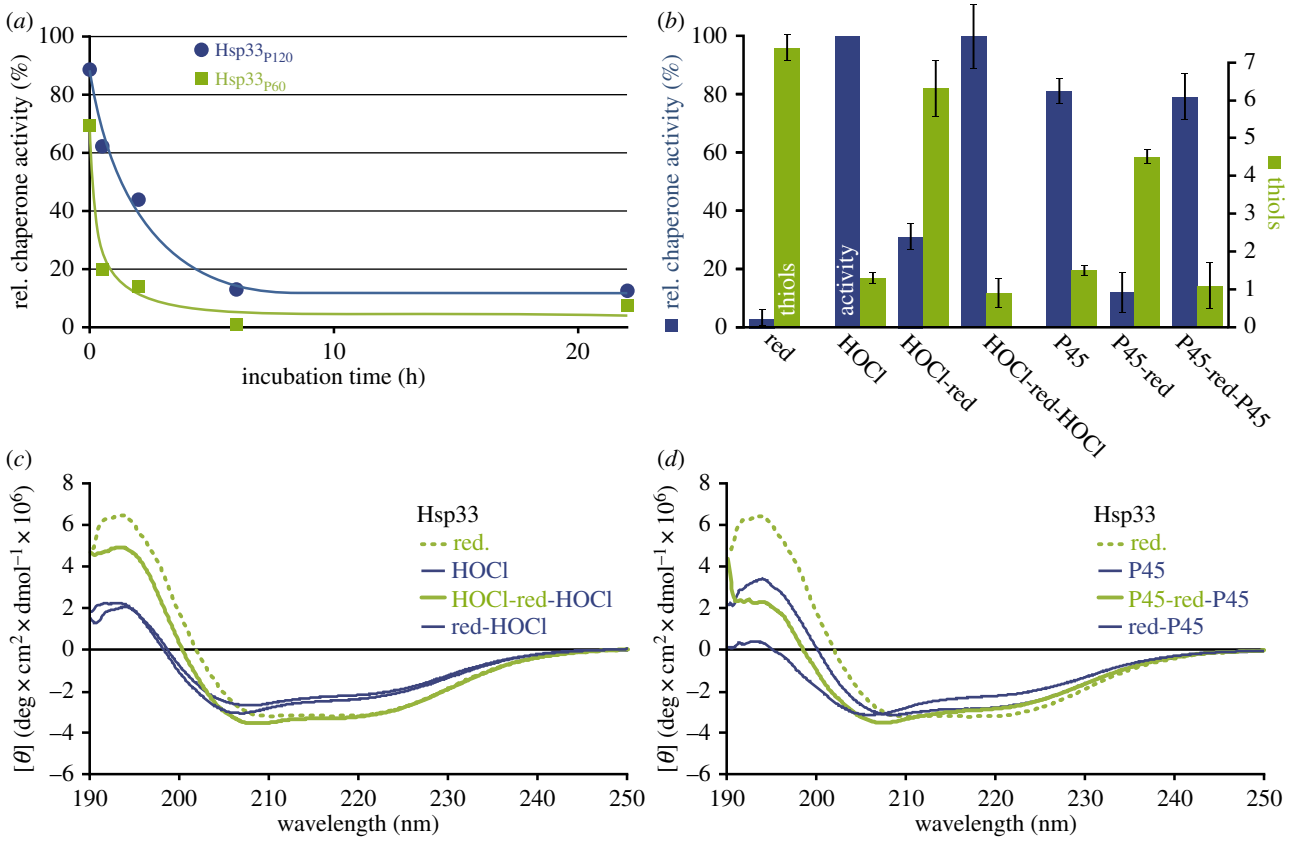

Figure 4. Investigation of the reversibility of plasma activation of Hsp33. (*a*) Inactivation kinetics of $Hsp33_{P60}$ and $Hsp33_{P120}$ incubated with DTT and $ZnCl_2$. (*b*) Activity (blue, left) and thiol oxidation status (green, right) of Hsp33 in the chaperone assay initially (red (abbreviation for reduced)), after activation with HOCl or plasma for 45 s (P45), inactivation by reduction (HOCl-red or P45-red, respectively), and a second activation by HOCl (HOCl-red-HOCl) or plasma (P45-red-P45). The data reflect at least three independent experiments. (*c*,*d*) CD spectra of Hsp33 after activation, inactivation and reactivation with HOCl (*c*) or plasma (*d*). (Online version in colour.)

figure S2), which could be due to the low HOCl concentration (electronic supplementary material, figure S1). The Hsp33 solution contains chloride ions stemming from the protein purification process. We removed the chloride ions by dialysis (confirmed by silver precipitation (electronic supplementary material, figure S3)) in order to limit HOCl production in the plasma-treated Hsp33 solution. There was no difference in chaperone activity in dialysed and non-dialysed samples after 60 s DBD treatment (electronic supplementary material, figure S2). Taken together, HOCl seems to play a minor role in plasma activation of Hsp33.

2.6. Importance of thiol oxidation for plasma activation of Hsp33

Having excluded HOCl as the main activating species, these results raised the intriguing question as to what other reactive species are generated by the plasma treatment that interacts with and activates Hsp33. Since plasma-treated chloride-containing buffer was unable to activate Hsp33 (electronic supplementary material, figure S2), we excluded that any other stable species that have previously been shown to form in the liquid (i.e. peroxynitrite) (electronic supplementary material, figure S4) are responsible for the activation of Hsp33. We also exclude that Hsp33 is activated by a combination of H_2O_2 and heat, since no warming of the sample occurred during plasma treatment with a similar set-up [41].

To unravel whether the unknown activator is oxygen-based or nitrogen-based, we treated Hsp33 with plasma as before but performed the treatment in an oxygen-free N_2/H_2-atmosphere (97.5%/2.5%). After a 60 s treatment in an oxygen-free atmosphere, we did not observe any significant activation of Hsp33 (electronic supplementary material, figure S2). It has been shown that the rates of hydroxyl radical formation by plasma-induced homolytic cleavage of water are of the same order of magnitude in the presence and absence of molecular oxygen [42,43]. Thus, these results excluded the involvement of hydroxyl radicals. These results are corroborated by an independent line of evidence. Hydroxyl radicals can also be formed in H_2O photodissociation by plasma-generated UV [44]. We mimicked the UV dose generated by the DBD using a UV lamp generating radiation of the same wavelength but with higher intensity. UV-exposed Hsp33 was not activated (electronic supplementary material, figure S2).

The fact that in oxygen-free atmosphere Hsp33 was not activated by plasma treatment suggested that molecular oxygen is crucial for the formation of the Hsp33-activating species. Possible short-living species generated by plasma operated with molecular oxygen are for instance atomic oxygen, superoxide, or singlet oxygen [45]. Based on the current data, we are not able to conclude which species is key to Hsp33 activation.

To investigate the importance of thiol modifications by plasma for activation of Hsp33 in more detail, we added two thiol-containing scavengers that affected Hsp33 activation in a concentration-dependent manner, glutathione (GSH) and DTT (figure 5*a*). The thiol groups of GSH and DTT either reduce plasma-oxidized Hsp33 or directly react with the activating species, outcompeting the Hsp33 thiols.

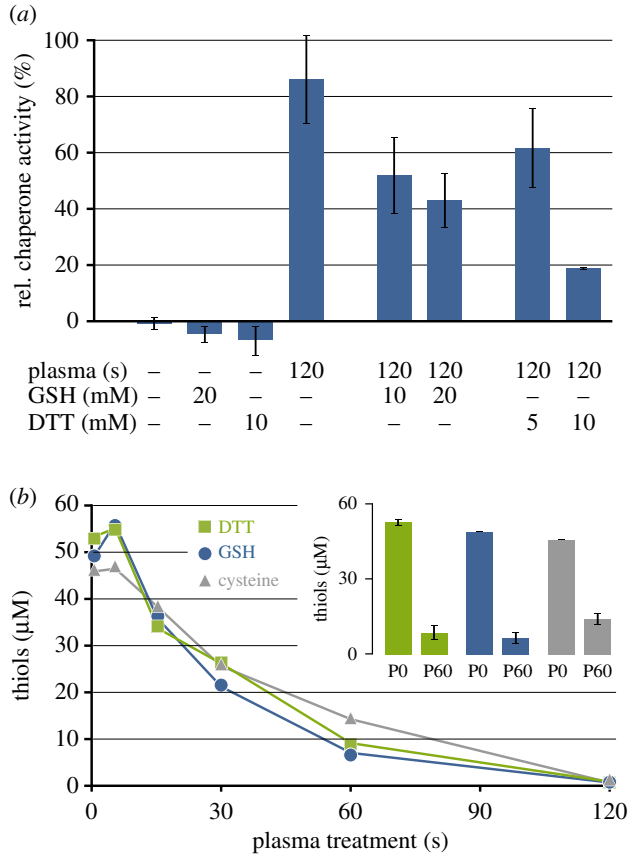

Figure 5. Influence of ROS scavengers GSH and DTT on Hsp33 activity and kinetics of scavenger oxidation by plasma. (*a*) Relative chaperone activity of Hsp33 after DBD plasma treatment in the absence or presence of GSH (10 or 20 mM) or DTT (5 or 10 mM). Data reflect three independent experiments. (*b*) Free thiols in 25 µM DTT, 50 µM GSH, or 50 µM cysteine after different plasma treatment times (compare to Hsp33 thiol oxidation in figure 3*b*). Insert: For DTT, GSH, or cysteine, free thiol quantitation for the untreated controls (P0) and the 60 s plasma treatment time point (P60) is shown with the data reflecting three independent experiments. (Online version in colour.)

Plasma-mediated oxidation of GSH has previously been described for a similar DBD set-up [10]. Exposure of GSH, DTT, or cysteine to DBD plasma and subsequent quantitation of free thiols revealed that all three oxidize very quickly, with similar half times for thiol oxidation (figure 5*b*) and at a rate comparable to that of the Hsp33 thiols (figure 3*b*). The results of the scavenging experiment underscore the importance of the thiol state for Hsp33 activity and make it likely that a thiol-oxidizing species is required for Hsp33 activation. GSH has been described to react with superoxide, H_2O_2, hydroxyl radicals, ozone, or NO• [10,46–48], and DTT is also known to react with H_2O_2, superoxide, or hydroxyl radicals [46,49]. To our knowledge, it is not known if they also react with atomic oxygen or singlet oxygen.

3. Discussion

Protein aggregation is known to occur in plasma-exposed cells [21]. The chaperone Hsp33 acts as a holdase that prevents protein aggregation under stress conditions [22,50]. In the present study, we investigated the influence of Hsp33 on bacterial plasma resistance using *E. coli* as a model. We further studied the effects of plasma on Hsp33 activity and protein fold and sought insights into plasma-specific activation mechanisms.

3.1. Role of Hsp33 in plasma protection

Vaze *et al.* exposed *E. coli* mutants with impairments in different chaperone systems (like GroEL, ClpX, and HtpG) to a DBD plasma. Under conditions that caused a 2 log reduction of the wild-type, deletion mutants lacking either of the chaperones were completely inactivated [51]. Here we showed that over-expression of the gene *hslO* encoding the chaperone Hsp33 increases plasma resistance of *E. coli*, while *hslO* deletion causes hypersensitivity (figure 1). Thus, Hsp33 conveys a clear benefit for surviving plasma exposure underscoring the importance of protein aggregation as a plasma-based antibacterial mechanism.

We have previously shown that the oxidation of proteins mediated by plasma occurs on the same timescale as protein aggregation. GapDH, for instance, is a key enzyme in the central metabolism with a catalytic cysteine residue that is heavily prone to oxidation. When treating bacteria with a microscale atmospheric-pressure plasma jet (µAPPJ), 1 min of treatment is sufficient for GapDH inactivation [17]. In the context of protective stress responses, it remains to be investigated whether plasma resistance of *E. coli* further increases when both the stress response to protein aggregating and protein oxidizing conditions are upregulated.

To investigate Hsp33 activity, we performed a gel-based *in vitro* protein aggregation assay with *E. coli* lysates into which Hsp33 was spiked prior to plasma treatment. Spiked Hsp33 delayed protein aggregation during plasma exposure (figure 2). However, it also showed that protein degradation occurs (figure 2) [52,53].

3.2. Hsp33 is reversibly activated by plasma

Most plasma-protein interactions analysed to date resulted in protein inactivation or denaturation [12,13,54,55]. The chaperone Hsp33 instead was activated by exposure to plasma, making this an interesting protein to study with regard to the protein activation mechanism.

During HOCl activation of Hsp33, the hydrophobic binding region of Hsp33 dissociates from its hydrophobic counterpart and binds to unfolded proteins, as they expose their hydrophobic 'cores' to the aqueous phase [56]. Like HOCl, plasma caused Hsp33 to unfold. When treated longer than 45 s, an extraordinary loss in secondary structures was observed by CD spectroscopy (see $Hsp33_{P120}$ in figure 3*c*). Such a degree of unfolding was not observed after HOCl or H_2O_2 treatment [24]. This highly unfolded Hsp33 did not aggregate, but stayed soluble and prevented chemically denatured citrate synthase from aggregating.

Activation of $Hsp33_{P45}$ was reversible when applying reducing conditions and supplying Zn^{2+} ions, and the Ellman's assay showed that oxidation of at least four of the six cysteine residues was reversible (figure 4*b*). Nevertheless, a 100% reduction of the cysteines of $Hsp33_{P45}$ could not be achieved with DTT. The formation of disulfide bonds (as observed for HOCl-activated Hsp33) or sulfenic acids (R-SOH) is reversible. Based on the Ellman's assay results, we speculate that, as described for GapDH or RNase A [15,17], the plasma causes oxidation of at least one cysteine residue of Hsp33 to sulfinic (R-SOOH) or sulfonic acids ($R\text{-}SO_2OH$) not reducible by DTT.

Reduction of $Hsp33_{P45}$ did not restore the initial fold of the protein and a second plasma exposure resulted in further loss of structural features in $Hsp33_{P45\text{-}red\text{-}P45}$ (figure 4*d*). The

degree of unfolding of the inactive $Hsp33_{P45\text{-}red}$ is comparable to that of $Hsp33_{P45}$ and $Hsp33_{HOCl}$. These findings are congruent with the model that unfolding alone is insufficient for Hsp33 activity and the thiol state is a co-determinant [23]. Thus, the plasma-activation mechanism differs from that of the lipase from *C. rugosa* for which it has been shown that protein activity correlates with the degree of plasma-induced unfolding [19]. Future studies using high-resolution mass spectrometry will reveal which amino acid residues are modified in plasma-activated versus bleach-activated Hsp33.

3.3. Investigation into plasma-generated activator(s)

In vitro, Hsp33 can be activated by H_2O_2 or NO• alongside elevated temperatures, •OH radicals, or HOCl [24,25]. Hydrogen peroxide and nitric oxide are both generated by plasmas interacting with liquids in ambient air [30,57]. However, for activation of Hsp33 by these species, an increased temperature of about 43°C is necessary, which is not reached within the treatment times with the device applied here [24,41]. Hydroxyl radicals can also activate Hsp33 *in vitro* [25]. The generation of •OH in plasma or in plasma-treated liquids is not oxygen-dependent, as for instance water molecules can either be split by free electrons or undergo photodissociation [42,44,45]. Hydroxyl radicals thus are generated in the presence and absence of molecular oxygen. Since no activation of Hsp33 was observed in an oxygen-free atmosphere or by treatment with high-intensity UV radiation, hydroxyl radicals do not seem to be the main activating factor.

Hypochlorous acid is a very potent activator of Hsp33 and its presence in plasma-treated solutions has been previously predicted and observed experimentally [31,58]. Thiol groups of zinc-finger motifs similar to the ones in Hsp33 have been shown to react with HOCl at very high rates close to being limited only by diffusion [59]. The fast reaction of HOCl with cysteines is congruent with effective scavenging with thiol-containing compounds (figure 5*b*). The concentrations of HOCl detected in this study in DBD-treated liquids (electronic supplementary material, figure S1) are too low to explain Hsp33 activation and no Hsp33 activity was observed when applying plasma-treated liquids.

However, when cysteine residues are oxidized by HOCl, the chloride ions are released after the formation of sulfenic acid (figure 6) [60]. It is conceivable that as long as atomic oxygen is supplied by plasma, the chloride ions repeatedly form HOCl, which rapidly reacts with the next cysteine residue. We have recently shown that plasma-generated atomic oxygen efficiently enters the liquid phase and is able to react there with dissolved organic compounds like phenol [32]. If plasma drives such a Cl^--HOCl cycle, due to the fast reaction rate of HOCl even small amounts of Cl^-, as present after dialysis, for instance, might be sufficient to oxidize Hsp33 during plasma treatment. In order to prove that HOCl is a main contributor, HOCl would need to be quantified during plasma treatment rather than post treatment in plasma-treated buffers. Unfortunately, HPF and APF are both not suitable for such direct measurements, since these probes seem to interact with plasma in a hitherto unknown manner. Other techniques for *in situ* HOCl determination need to be established.

Other species to consider as Hsp33 activators are superoxide, atomic oxygen, and singlet oxygen. Singlet oxygen has been shown to interact with zinc-finger cysteines [61].

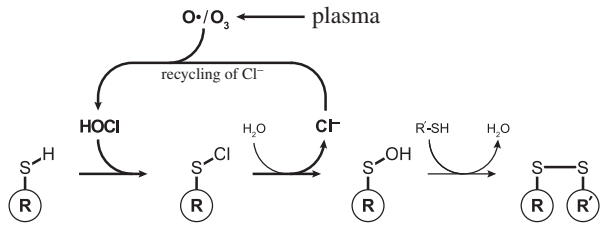

Figure 6. Plasma-driven Cl^--HOCl cycle: the reaction of thiol groups with HOCl results in the formation of disulfide bonds. Released chloride ions can re-react with plasma-supplied atomic oxygen or ozone to form HOCl again (according to Gray *et al.* [60]).

Its formation in plasma is O_2-dependent, as is the generation of atomic oxygen [45,62]. Since all samples were placed between the electrodes, they were exposed to the electric field. It will be interesting if the electric field has an influence on Hsp33 activation.

In conclusion, based on the data, we expect short-living thiol-reactive species to be responsible for plasma activation of Hsp33.

3.4. Plasmas in clinical application

Plasma is composed of a very dynamic mixture of reactive species. Proteins like Hsp33 that are not only activated by plasma treatment but also protect other cellular proteins from plasma-induced protein aggregation and can contribute to plasma resistance in bacteria. Although elevated levels of Hsp33 alone increased plasma resistance only marginally, a combination with other bacterial stress protection mechanisms [63] might result in bacterial strains with plasma resistance comparable to that of eukaryotic cells. This would limit future applications in the medical field that exploit the higher plasma susceptibility of bacteria. In this study, overproduction of Hsp33 was achieved experimentally by over-expression of *hslO*. However, similar effects on protein levels can result from naturally occurring mutations of promotors (the regulatory region of genes) or in genes encoding regulators.

4. Material and methods

4.1. Plasma sources

A portable dielectric barrier discharge (DBD) plasma source (Soft Bond, Hollywood Nails, Remscheid, Germany) was applied for all plasma treatments. The driven copper electrode has a diameter of 7.8 mm and is covered by an Al_2O_3 dielectric. Plasma was ignited with 10–11 kV_{pp} and 289 Hz using ambient air as process gas, if not indicated otherwise. Samples were placed on glass slides on a grounded metal electrode. The distance between the driven electrode and the samples was 1 mm.

4.2. Survival rate assay

For determination of the plasma sensitivity, cultures of *E. coli* BW25113 (parent strain), BW25113 pCA24N, BW25113 Δ*hslO* (JW5692) [34], Δ*hslO* pCA24N and Δ*hslO* pCA24N::*hslO* [35] were inoculated with an overnight pre-culture and grown under steady agitation at 37°C in LB medium [64]. Kanamycin (50 μg ml^{-1}) or chloramphenicol (50 μg ml^{-1}) was added, when needed. For induction of episomally encoded *hslO*, different amounts of isopropyl thiogalactopyranoside (IPTG) were added directly when the main culture was inoculated. When

$OD_{600} = 0.3$ was reached, cells were diluted 1 : 15 000 in LB medium. For plasma treatment, 5 µl of the cell suspension were placed onto glass slides and exposed to DBD plasma for 30 s. Afterwards, cells were washed off the slide applying two times 100 µl NaCl (0.9% (w/v)) and the recovered 205 µl were plated on LB agar. After incubation overnight at 37°C colonies were counted. Controls were processed in the same manner without ignition of the plasma. Western blot analysis was performed according to standard protocols [65] using penta-His HRP-conjugated antibodies (Qiagen, Hilden, Germany).

4.3. Protein aggregation of cell lysate

For the preparation of cell lysate, a culture of *E. coli* BB7222 [66] grown overnight in LB medium was harvested by centrifugation and resuspended in cell lysate buffer (50 mM Tris, 175 mM KCl, and 1 mM $MgCl_2$, pH 8). Cell disruption was performed by sonication. After centrifugation at 21 000*g* and 4°C for 45 min, the protein concentration of the supernatant was determined by Bradford assay [67]. The concentration was adjusted to 5 mg ml^{-1}. Purified Hsp33 was added to a final concentration of 16% (w/w) when indicated. Aliquots of 8 µl of cell lysate were treated with plasma for different amounts of time and recovered until a final volume of 15 µl was reached. Soluble and insoluble fractions were separated by centrifugation (21 000*g* at 4°C for 45 min) to distinguish between native and denatured proteins. Pellets containing denatured proteins were washed once with cell lysate buffer. Both, soluble and insoluble fractions were then subjected to SDS-PAGE and Bradford assay [65]. To solubilize the denatured proteins for Bradford analyses, the pellet was resuspended in lysate buffer containing 6 M urea [68]. The samples were heated to 100°C for 10 min and protein concentration determined.

4.4. Hsp33 preparation and treatment

Wild-type Hsp33 was purified as described by Jakob *et al.* [50]. Briefly, high-density and arabinose-induced cultures of *E. coli* BB7222 pBAD30::*hslO* were disrupted by sonication and the cell-free lysate subjected to anion-exchange, hydroxyapatite, and size-exclusion chromatography. In the last chromatographic purification step (size-exclusion chromatography), Hsp33 was eluted with potassium phosphate buffer (40 mM, pH 7.5) containing 200 mM KCl. The protein was diluted 1 : 10 in potassium phosphate buffer (40 mM, pH 7.5) and concentrated with centrifugal filter units (cut-off 10 kDa). For the generation of chloride-depleted Hsp33, 400 µl of an Hsp33 solution was dialysed consecutively against 2 l and 1 l chloride-free phosphate buffer at 4°C overnight.

Reduction of Hsp33 ($Hsp33_{red}$) was performed by adding 5 mM dithiothreitol (DTT) and 240 µM $ZnCl_2$ to 300 µM Hsp33 (for dialysed samples $ZnSO_4$ was substituted for $ZnCl_2$). The mixture was incubated at 37°C for at least 1.5 h [27]. For analysis of reversibility of Hsp33 activation, the concentrations of Hsp33, DTT and Zn^{2+} were scaled up linearly to 900 µM Hsp33.

The term HOCl is used here to describe sodium hypochlorite (Sigma-Aldrich, St Louis, MO, USA), which was diluted in water yielding an equimolar mixture of hypochlorous acid (HOCl) and its conjugate base (OCl^-). HOCl-oxidized Hsp33 ($Hsp33_{HOCl}$) was prepared by incubation of $Hsp33_{red}$ with 10-fold molar excess of HOCl under steady agitation at 30°C for 5 min.

After each reduction or oxidation with HOCl, the reductants, oxidants, and small molecules were removed using NAP-5-columns (GE Healthcare, Chalfont St Giles, UK) or Micro Bio-Spin Chromatography Columns (Bio-Rad, Munich, Germany) according to manufacturers' instructions.

To prepare plasma-treated Hsp33 ($Hsp33_{Px}$, where *x* indicates the treatment time in seconds), 5 µl aliquots of $Hsp33_{red}$ (150 µM) were spotted onto glass coverslips and exposed to plasma for up to 120 s. After recovering the solution from the coverslip, aliquots were pooled.

DTT (5 and 10 mM) or glutathione (GSH, 10 and 20 mM) were added to $Hsp33_{red}$ as scavengers before plasma treatment to analyse their influence on Hsp33 activation.

4.5. Chaperone activity assay

Hsp33 chaperone activity was determined as described by Ilbert *et al.* [28]. Citrate synthase (Sigma-Aldrich) was denatured chemically by incubation in 4.5 M guanidinium chloride (in 40 mM HEPES, pH 7.5) for at least 2 h. For chaperone activity assay, denatured citrate synthase was diluted in reaction buffer (40 mM HEPES, pH 7.5) containing four times the amount of Hsp33 in a quartz cuvette to a final volume of 1.6 ml. The assay was performed at 25°C and stirred with 800 r.p.m. The increase in light scattering by aggregating citrate synthase was monitored using a fluorescence spectrometer (FP-8500, Jasco, Gross-Umstadt, Germany). The intensity after 4 min incubation was used to calculate chaperone activity. Scattering of samples without Hsp33 was set to 0%, while $Hsp33_{HOCl}$ was set to 100%.

4.6. Circular dichroism spectroscopy

Far-UV-CD spectroscopy was carried out with a Jasco J-815 spectropolarimeter in a quartz cuvette with 1 mm path length at 25°C. Hsp33 was diluted to 0.15–0.2 mg ml^{-1} for measurements. Spectra were buffer-corrected, normalized to protein concentration and converted to molar ellipticity as described by Graf *et al.* [23]. Each spectrum shown here is a representative of at least three repeat experiments starting from Hsp33 from two independent purifications.

4.7. Determination of Hsp33 oxidation state

The oxidation state of the cysteine residues of Hsp33 was determined by Ellman's assay [36]. Hsp33 was diluted to 5–10 µM and incubated with 16.7 mM 5,5′-dithiobis-(2-nitrobenzoic acid) (DTNB) and 6 M guanidinium chloride in potassium phosphate buffer (40 mM, pH 7.5) at room temperature for 15 min. Afterwards, absorption at 412 nm was determined. The overall number of thiols was calculated by application of Beer–Lambert Law, ($\varepsilon_{412} = 13\,880\ M^{-1}\ cm^{-1}$). Determination of free thiols of DTT, GSH, and cysteine was performed accordingly.

4.8. Reversibility of $Hsp33_{Px}$ activation

For analysis of the reversibility of plasma-activated Hsp33, $Hsp33_{HOCl}$ or $Hsp33_{Px}$ were diluted to 5 µM and incubated with 5 mM DTT and 5 µM $ZnCl_2$ at 30°C for up to 22 h yielding $Hps33_{HOCl\text{-}red}$ or $Hsp33_{Px\text{-}red}$, respectively [24]. At several time points, aliquots were subjected to chaperone activity assay. After 22 h, reducing agents and small molecules were removed as described previously. Subsequently, both variants were reactivated ($Hsp33_{HOCl\text{-}red\text{-}HOCl}$ or $Hsp33_{Px\text{-}red\text{-}Px}$). Aliquots of all interim steps were subjected to chaperone activity assay, CD spectroscopy, and quantification of free thiols.

4.9. Effect of UV radiation

Treatment of $Hsp33_{red}$ with UV radiation was performed using a calibrated Hamamatsu L98417 UV lamp (Hamamatsu Photonics, Hamamatsu City, Japan) combined with a UV-C cut-off filter. The distance between the lamp and the sample was adjusted to yield 0.4 mW m^{-2}. A run time of 30 s with this set-up produced a UV dose comparable to 120 s of treatment with the DBD [69].

4.10. HOCl determination

Fifty microlitres of potassium phosphate buffer (40 mM, pH 7.5) with or without 20 mM KCl were exposed to DBD for different amounts of time. Directly after treatment, 50 µl of either HPF or APF solution (10 µM) was added [37]. After 30 min incubation at room temperature, fluorescence intensities were measured using $\lambda_{ex} = 490$ nm and $\lambda_{em} = 515$ nm. The amount of HOCl generated was calculated according to the following equation:

$$[\mathrm{HOCl}] = {}^{+}\mathrm{APF} - {}^{+}\mathrm{HPF} \times \frac{{}^{-}\mathrm{APF}}{{}^{-}\mathrm{HPF}} \times 8.5,$$

whereby $^{+}$XPF is the fluorescence intensity of HPF or APF in chloride-containing buffer and $^{-}$XPF is the fluorescence intensity of HPF or APF in chloride-free buffer. Untreated buffers were used as reference. The multiplication factor 8.5 is used to convert the HOCl concentration from a 50 µl sample volume to a volume of 5 µl as used for Hsp33 treatment. This procedure was necessary because the fluorescence signal changes over time and treatment of small volumes with subsequent pooling of the samples was not possible. Further, the minimal volume for measurements with the applied equipment was 100 µl. Therefore, H_2O_2 generation was monitored and used for recalculating the difference in treated volumes (multiplication factor 8.5), because along with HOCl, H_2O_2 is one of the most stable species generated by plasma–liquid interaction. The multiplication factor was determined by quantifying H_2O_2 concentrations using the $TiO(SO_4)$ assay after exposing different volumes of potassium phosphate buffer (40 mM, pH 7.5) to plasma for 1 min (electronic supplementary material, figure S5) [70,71].

The intensities achieved for the probe HPF were used for calculation of peroxynitrite concentrations in the plasma-treated buffers assuming hydroxyl radicals to decay completely between plasma treatment und addition of HPF. Peroxynitrite for calibration was freshly synthesized from isoamyl nitrite and hydrogen peroxide [72].

4.11. Chloride ion determination

Chloride ions in solution were quantified by precipitating Cl^- with silver ions. To the samples, final concentrations of 50 mM HNO_3 and 20 mM $AgNO_3$ were added and the solutions mixed vigorously. Formation of white AgCl precipitate was analysed photometrically at 315 nm. By calibration with different concentrations of KCl, the detection limit was determined to be 20 µM Cl^-. In the case of Hsp33-containing samples, the protein was removed prior to Cl^- determination with molecular weight cut-off centrifugal filter units (3 kDa).

Data accessibility. Electronic supplementary material is available online at https://dx.doi.org/10.6084/m9.figshare.c.4531724.

Authors' contributions. M.K. performed experiments, analysed data, participated in study design and wrote the manuscript. J.J.S. performed experiments, analysed data and participated in study design. C.C. contributed to experiments and data analysis. J.-W.L. participated in data analysis and study design. B.S. performed experiments. P.A. provided material and plasma expertise. L.I.O.L. provided instruments and analysed data. U.J. participated in the conception of the study, study design and data analysis. J.E.B. conceived, designed and coordinated the study and wrote the manuscript. All authors gave final approval for publication.

Competing interests. Authors declare no competing interests.

Funding. J.E.B., P.A., and L.I.L. gratefully acknowledge funding from the German Research Foundation (J.E.B.: BA 4193/7-1, P.A. and J.E.B.: CRC 1316-1, and L.I.L.: LE2905/1-2). J.S. received a PROMOS mobility stipend from the German Academic Exchange Service (DAAD).

Acknowledgements. We thank Christian Herrmann for access to the CD spectrometer.

References

1. Weltmann K-D, Brandenburg R, Woedtke T, Ehlbeck J, Foest R, Stieber M, Kindel E. 2008 Antimicrobial treatment of heat sensitive products by miniaturized atmospheric pressure plasma jets (APPJs). *J. Phys. D: Appl. Phys.* **41**, 194008. (doi:10.1088/0022-3727/41/19/194008)
2. Brandenburg R, Ehlbeck J, Stieber M, Woedtke T, Zeymer J, Schlüter O, Weltmann K-D. 2007 Antimicrobial treatment of heat sensitive materials by means of atmospheric pressure Rf-driven plasma jet. *Contrib. Plasma Phys.* **47**, 72–79. (doi:10.1002/ctpp.200710011)
3. Haertel B, Woedtke T, Weltmann K-D, Lindequist U. 2014 Non-thermal atmospheric-pressure plasma possible application in wound healing. *Biomol. Ther.* **22**, 477–490. (doi:10.4062/biomolther.2014.105)
4. Fridman G, Friedman G, Gutsol A, Shekhter AB, Vasilets VN, Fridman A. 2008 Applied plasma medicine. *Plasma Process. Polym.* **5**, 503–533. (doi:10.1002/ppap.200700154)
5. Graves DB. 2012 The emerging role of reactive oxygen and nitrogen species in redox biology and some implications for plasma applications to medicine and biology. *J. Phys. D: Appl. Phys.* **45**, 263001. (doi:10.1088/0022-3727/45/26/263001)
6. Choi S, Attri P, Lee I, Oh J, Yun J-H, Park JH, Choi EH, Lee W. 2017 Structural and functional analysis of lysozyme after treatment with dielectric barrier discharge plasma and atmospheric pressure plasma jet. *Sci. Rep.* **7**, 115012. (doi:10.1038/s41598-017-01030-w)
7. Privat-Maldonado A, O'Connell D, Welch E, Vann R, van der Woude MW. 2016 Spatial dependence of DNA damage in bacteria due to low-temperature plasma application as assessed at the single cell level. *Sci. Rep.* **6**, 918. (doi:10.1038/srep35646)
8. Dolezalova E, Lukes P. 2015 Membrane damage and active but nonculturable state in liquid cultures of *Escherichia coli* treated with an atmospheric pressure plasma jet. *Bioelectrochemistry* **103**, 7–14. (doi:10.1016/j.bioelechem.2014.08.018)
9. Li Y, Friedman G, Fridman A, Ji H-F. 2014 Decomposition of sugars under non-thermal dielectric barrier discharge plasma. *Clin. Plasma Med.* **2**, 56–63. (doi:10.1016/j.cpme.2014.08.001)
10. Klinkhammer C, Verlackt C, Śmiłowicz D, Kogelheide F, Bogaerts A, Metzler-Nolte N, Stapelmann K, Havenith M, Lackmann J-W. 2017 Elucidation of plasma-induced chemical modifications on glutathione and glutathione disulphide. *Sci. Rep.* **7**, 196. (doi:10.1038/s41598-017-13041-8)
11. Takai E, Kitano K, Kuwabara J, Shiraki K. 2011 Protein inactivation by low-temperature atmospheric pressure plasma in aqueous solution. *Plasma Process Polym.* **9**, 77–82. (doi:10.1002/ppap.201100063)
12. Zhang H *et al*. 2015 Effects and mechanism of atmospheric-pressure dielectric barrier discharge cold plasma on lactate dehydrogenase (LDH) enzyme. *Sci. Rep.* **5**, 323001. (doi:10.1038/srep10031)
13. Pankaj SK, Misra NN, Cullen PJ. 2013 Kinetics of tomato peroxidase inactivation by atmospheric pressure cold plasma based on dielectric barrier discharge. *Innov. Food Sci. Emerg.* **19**, 153–157. (doi:10.1016/j.ifset.2013.03.001)
14. Ke Z, Huang Q. 2013 Inactivation and heme degradation of horseradish peroxidase induced by discharge plasma. *Plasma Process Polym.* **10**, 731–739. (doi:10.1002/ppap.201300035)
15. Lackmann J-W *et al*. 2015 A dielectric barrier discharge terminally inactivates RNase A by oxidizing sulfur-containing amino acids and breaking structural disulfide bonds. *J. Phys. D: Appl. Phys.* **48**, 494003. (doi:10.1088/0022-3727/48/49/494003)
16. Alkawareek MY, Gorman SP, Graham WG, Gilmore BF. 2014 Potential cellular targets and antibacterial efficacy of atmospheric pressure non-thermal

plasma. *Int. J. Antimicrob. Agents* **43**, 154–160. (doi:10.1016/j.ijantimicag.2013.08.022)

17. Lackmann J-W, Schneider S, Edengeiser E, Jarzina F, Brinckmann S, Steinborn E, Havenith M, Benedikt J, Bandow JE. 2013 Photons and particles emitted from cold atmospheric-pressure plasma inactivate bacteria and biomolecules independently and synergistically. *J. R. Soc. Interface* **10**, 20130591. (doi:10.1098/rsif.2013.0591)
18. Takai E, Kitamura T, Kuwabara J, Ikawa S, Yoshizawa S, Shiraki K, Kawasaki H, Arakawa R, Kitano K. 2014 Chemical modification of amino acids by atmospheric-pressure cold plasma in aqueous solution. *J. Phys. D: Appl. Phys.* **47**, 285403. (doi:10.1088/0022-3727/47/28/285403)
19. Li H-P, Wang L-Y, Li G, Jin L-H, Le P-S, Zhao H-X, Xing X-H, Bao C-Y. 2011 Manipulation of lipase activity by the helium radio-frequency, atmospheric-pressure glow discharge plasma jet. *Plasma Process Polym.* **8**, 224–229. (doi:10.1002/ppap.201000035)
20. Bednarska NG, Schymkowitz J, Rousseau F, Van Eldere J. 2013 Protein aggregation in bacteria: the thin boundary between functionality and toxicity. *Microbiology* **159**, 1795–1806. (doi:10.1099/mic.0.069575-0)
21. Itooka K, Takahashi K, Kimata Y, Izawa S. 2018 Cold atmospheric pressure plasma causes protein denaturation and endoplasmic reticulum stress in *Saccharomyces cerevisiae*. *Appl. Microbiol. Biotechnol.* **102**, 2279–2288. (doi:10.1007/s00253-018-8758-2)
22. Winter J, Linke K, Jatzek A, Jakob U. 2005 Severe oxidative stress causes inactivation of DnaK and activation of the redox-regulated chaperone Hsp33. *Mol. Cell* **17**, 381–392. (doi:10.1016/j.molcel.2004.12.027)
23. Graf PCF, Martinez-Yamout M, VanHaerents S, Lilie H, Dyson HJ, Jakob U. 2004 Activation of the redox-regulated chaperone Hsp33 by domain unfolding. *J. Biol. Chem.* **279**, 20 529–20 538. (doi:10.1074/jbc.M401764200)
24. Winter J, Ilbert M, Graf PCF, Ozcelik D, Jakob U. 2008 Bleach activates a redox-regulated chaperone by oxidative protein unfolding. *Cell* **135**, 691–701. (doi:10.1016/j.cell.2008.09.024)
25. Jakob U, Eser M, Bardwell J. 2000 Redox switch of Hsp33 has a novel zinc-binding motif. *J. Biol. Chem.* **275**, 38 302–38 310. (doi:10.1074/jbc.M005957200)
26. Won H-S, Low LY, De Guzman R, Martinez-Yamout M, Jakob U, Jane Dyson H. 2004 The zinc-dependent redox switch domain of the chaperone Hsp33 has a novel fold. *J. Mol. Biol.* **341**, 893–899. (doi:10.1016/j.jmb.2004.06.046)
27. Graumann J, Lilie H, Tang XL, Tucker KA, Hoffmann JT, Vijayalakshmi J, Saper M, Bardwell J, Jakob U. 2001 Activation of the redox-regulated molecular chaperone Hsp33—a two-step mechanism. *Structure* **9**, 377–387. (doi:10.1016/S0969-2126(01)00599-8)
28. Ilbert M, Horst J, Ahrens S, Winter J, Graf PCF, Lilie H, Jakob U. 2007 The redox-switch domain of Hsp33 functions as dual stress sensor. *Nat. Struct. Mol. Biol.* **14**, 556–563. (doi:10.1038/nsmb1244)
29. Laroussi M, Leipold F. 2004 Evaluation of the roles of reactive species, heat, and UV radiation in the inactivation of bacterial cells by air plasmas at atmospheric pressure. *Int. J. Mass. Spectrom.* **233**, 81–86. (doi:10.1016/j.ijms.2003.11.016)
30. Bruggeman PJ *et al*. 2016 Plasma–liquid interactions: a review and roadmap. *Plasma Sources Sci. Technol.* **25**, 053002. (doi:10.1088/0963-0252/25/5/053002)
31. Bekeschus S, Wende K, Hefny MM, Rödder K, Jablonowski H, Schmidt A, Woedtke TV, Weltmann K-D, Benedikt J. 2017 Oxygen atoms are critical in rendering THP-1 leukaemia cells susceptible to cold physical plasma-induced apoptosis. *Sci. Rep.* **7**, 263001. (doi:10.1038/s41598-017-03131-y)
32. Hefny MM, Pattyn C, Lukes P, Benedikt J. 2016 Atmospheric plasma generates oxygen atoms as oxidizing species in aqueous solutions. *J. Phys. D: Appl. Phys.* **49**, 404002. (doi:10.1088/0022-3727/49/40/404002)
33. Benedikt J, Mokhtar Hefny M, Shaw A, Buckley BR, Iza F, Schäkermann S, Bandow JE. 2018 The fate of plasma-generated oxygen atoms in aqueous solutions: non-equilibrium atmospheric pressure plasmas as an efficient source of atomic $O_{(aq)}$. *Phys. Chem. Chem. Phys.* **20**, 12 037–12 042. (doi:10.1039/C8CP00197A)
34. Baba T *et al*. 2006 Construction of *Escherichia coli* K-12 in-frame, single-gene knockout mutants: the KEIO collection. *Mol. Syst. Biol.* **2**, 2006.0008. (doi:10.1038/msb4100050)
35. Kitagawa M, Ara T, Arifuzzaman M, Ioka-Nakamichi T, Inamoto E, Toyonaga H, Mori H. 2005 Complete set of ORF clones of *Escherichia coli* ASKA library (a complete set of *E. coli* K-12 ORF archive): unique resources for biological research. *DNA Res.* **12**, 291–299. (doi:10.1093/dnares/dsi012)
36. Ellman GL. 1959 Tissue sulfhydryl groups. *Arch. Biochem. Biophys.* **82**, 70–77. (doi:10.1016/0003-9861(59)90090-6)
37. Setsukinai K-I, Urano Y, Kakinuma K, Majima HJ, Nagano T. 2003 Development of novel fluorescence probes that can reliably detect reactive oxygen species and distinguish specific species. *J. Biol. Chem.* **278**, 3170–3175. (doi:10.1074/jbc.M209264200)
38. Kanofsky JR. 2011 Measurement of singlet-oxygen *in vivo*: progress and pitfalls. *Photochem. Photobiol.* **87**, 14–17. (doi:10.1111/j.1751-1097.2010.00855.x)
39. Hibert C, Gaurand I, Motret O, Pouvesle JM. 1999 [OH(X)] measurements by resonant absorption spectroscopy in a pulsed dielectric barrier discharge. *J. Appl. Phys.* **85**, 7070–7075. (doi:10.1063/1.370514)
40. Ishihara M, Murakami K, Fukuda K, Nakamura S, Kuwabara M, Hattori H, Fujita M, Kiyosawa T, Yokoe H. 2017 Stability of weakly acidic hypochlorous acid solution with microbicidal activity. *Biocontrol. Sci.* **22**, 223–227. (doi:10.4265/bio.22.223)
41. Kuchenbecker M, Bibinov N, Kaemlimg A, Wandke D, Awakowicz P, Viöl W. 2009 Characterization of DBD plasma source for biomedical applications. *J. Phys. D: Appl. Phys.* **42**, 045212. (doi:10.1088/0022-3727/42/4/045212)
42. Bruggeman P, Schram DC. 2010 On OH production in water containing atmospheric pressure plasmas. *Plasma Sources Sci. Technol* **19**, 045025. (doi:10.1088/0963-0252/19/4/045025)
43. Sankaranarayanan R, Pashaie B, Dhali SK. 2000 Laser-induced fluorescence of OH radicals in a dielectric barrier discharge. *Appl. Phys. Lett.* **77**, 2970–2972. (doi:10.1063/1.1324002)
44. Attri P, Kim YH, Park DH, Park JH, Hong YJ, Uhm HS, Kim K.-N., Fridman A, Choi EH. 2015 Generation mechanism of hydroxyl radical species and its lifetime prediction during the plasma-initiated ultraviolet (UV) photolysis. *Sci. Rep.* **5**, 115020. (doi:10.1038/srep09332)
45. Sakiyama Y, Graves DB, Chang H-W, Shimizu T, Morfill GE. 2012 Plasma chemistry model of surface microdischarge in humid air and dynamics of reactive neutral species. *J. Phys. D: Appl. Phys.* **45**, 425201. (doi:10.1088/0022-3727/45/42/425201)
46. De Lamirande E, Gagnon C. 1992 Reactive oxygen species and human spermatozoa. I. Effects on the motility of intact spermatozoa and on sperm axonemes. *J. Androl.* **13**, 368–378.
47. Chen QL, Olashaw N, Wu J. 1995 Participation of reactive oxygen species in the lysophosphatidic acid-stimulated mitogen-activated protein kinase kinase activation pathway. *J. Biol. Chem.* **270**, 28 499–28 502. (doi:10.1074/jbc.270.48.28499)
48. Wang SY, Jiao HJ. 2000 Scavenging capacity of berry crops on superoxide radicals, hydrogen peroxide, hydroxyl radicals, and singlet oxygen. *J. Agric. Food Chem.* **48**, 5677–5684. (doi:10.1021/jf000766i)
49. Halliwell B. 1981 Chloroplast metabolism. The structure and function of chloroplasts in green leaf cells. In *Chloroplast metabolism*. New York, NY: Oxford University Press.
50. Jakob U, Muse W, Eser M, Bardwell J. 1999 Chaperone activity with a redox switch. *Cell* **96**, 341–352. (doi:10.1016/S0092-8674(00)80547-4)
51. Vaze ND, Park S, Brooks AD, Fridman A, Joshi SG. 2017 Involvement of multiple stressors induced by non-thermal plasma-charged aerosols during inactivation of airborne bacteria. *PLoS ONE* **12**. e0171434 (doi:10.1371/journal.pone.0171434)
52. Deng XT, Shi JJ, Kong MG. 2007 Protein destruction by a helium atmospheric pressure glow discharge: capability and mechanisms. *J. Appl. Phys.* **101**, 074701-10. (doi:10.1063/1.2717576)
53. Bayliss DL, Walsh JL, Shama G, Iza F, Kong MG. 2009 Reduction and degradation of amyloid aggregates by a pulsed radio-frequency cold atmospheric plasma jet. *New J. Phys.* **11**. 115024. (doi:10.1088/1367-2630/11/11/115024)
54. Lee HJ, Shon CH, Kim YS, Kim S, Kim GC, Kong MG. 2009 Degradation of adhesion molecules of G361 melanoma cells by a non-thermal atmospheric pressure microplasma. *New J. Phys.* **11**, 115026. (doi:10.1088/1367-2630/11/11/115026)

55. Julák J, Janoušková, O., Scholtz V, Holada K. 2011 Inactivation of prions using electrical DC discharges at atmospheric pressure and ambient temperature. *Plasma Process Polym.* **8**, 316–323. (doi:10.1002/ppap.201000100)
56. Cremers CM, Reichmann D, Hausmann J, Ilbert M, Jakob U. 2010 Unfolding of metastable linker region is at the core of Hsp33 activation as a redox-regulated chaperone. *J. Biol. Chem.* **285**, 11 243–11 251. (doi:10.1074/jbc.M109.084350)
57. Baldus S, Schröder D, Bibinov N, Schulz-von der Gathen V, Awakowicz P. 2015 Atomic oxygen dynamics in an air dielectric barrier discharge: a combined diagnostic and modeling approach. *J. Phys. D: Appl. Phys.* **48**, 275203. (doi:10.1088/0022-3727/48/27/275203)
58. Wende K *et al*. 2015 Identification of the biologically active liquid chemistry induced by a nonthermal atmospheric pressure plasma jet. *Biointerphases* **10**, 029518. (doi:10.1116/1.4919710)
59. Lebrun V, Ravanat J-L, Latour J-M, Sénèque O. 2016 Near diffusion-controlled reaction of a $Zn(Cys)_4$ zinc finger with hypochlorous acid. *Chemical Science* **7**, 5508–5516. (doi:10.1039/C6SC00974C)
60. Gray MJ, Wholey W-Y, Jakob U. 2013 Bacterial responses to reactive chlorine species. *Annu. Rev. Microbiol.* **67**, 141–160. (doi:10.1146/annurev-micro-102912-142520)
61. Lebrun V, Tron A, Scarpantonio L, Lebrun C, Ravanat J-L, Latour J-M., McClenaghan ND, Sénèque O. 2014 Efficient oxidation and destabilization of $Zn(Cys)_4$ zinc fingers by singlet oxygen. *Angew. Chem. Int. Ed. Engl.* **53**, 9365–9368. (doi:10.1002/anie.201405333)
62. Ellerweg D, Benedikt J, Keudell A, Knake N, Schulz-von der Gathen V. 2010 Characterization of the effluent of a He/O_2 microscale atmospheric pressure plasma jet by quantitative molecular beam mass spectrometry. *New J. Phys.* **12**, 013021. (doi:10.1088/1367-2630/12/1/013021)
63. Mai-Prochnow A, Bradbury M, Ostrikov K, Murphy AB. 2015 *Pseudomonas aeruginosa* biofilm response and resistance to cold atmospheric pressure plasma is linked to the redox-active molecule phenazine. *PLoS ONE* **10**, e0130373. (doi:10.1371/journal.pone.0130373)
64. Bertani G. 1951 Studies on lysogenesis. I. The mode of phage liberation by lysogenic *Escherichia coli*. *J. Bacteriol.* **62**, 293–300.
65. Sambrook J, Russell DW. 2001 *Molecular cloning: a laboratory manual*, 3rd edn. New York, NY: CSHL Press.
66. Tomoyasu T, Mogk A, Langen H, Goloubinoff P, Bukau B. 2001 Genetic dissection of the roles of chaperones and proteases in protein folding and degradation in the *Escherichia coli* cytosol. *Mol. Microbiol.* **40**, 397–413. (doi:10.1046/j.1365-2958.2001.02383.x)
67. Bradford MM. 1976 A rapid and sensitive method for the quantitation of microgram quantities of protein utilizing the principle of protein–dye binding. *Anal. Biochem.* **72**, 248–254. (doi:10.1016/0003-2697(76)90527-3)
68. Gotham SM, Fryer PJ, Paterson WR. 1988 The measurement of insoluble proteins using a modified Bradford assay. *Anal. Biochem.* **173**, 353–358. (doi:10.1016/0003-2697(88)90199-6)
69. Rajasekaran P, Oplaender C, Hoffmeister D, Bibinov N, Suschek CV, Wandke D, Awakowicz P. 2011 Characterization of dielectric barrier discharge (DBD) on mouse and histological evaluation of the plasma-treated tissue. *Plasma Process Polym.* **8**, 246–255. (doi:10.1002/ppap.201000122)
70. Eisenberg G. 1943 Colorimetric determination of hydrogen peroxide. *Ind. Eng. Chem. Anal. Ed.* **15**, 327–328. (doi:10.1021/i560117a011)
71. Machala Z, Tarabova B, Hensel K, Spetlikova E, Sikurova L, Lukes P. 2013 Formation of ROS and RNS in water electro-sprayed through transient spark discharge in air and their bactericidal effects. *Plasma Process Polym.* **10**, 649–659. (doi:10.1002/ppap.201200113)
72. Uppu RM, Pryor WA. 1996 Synthesis of peroxynitrite in a two-phase system using isoamyl nitrite and hydrogen peroxide. *Anal. Biochem.* **236**, 242–249. (doi:10.1006/abio.1996.0162)